AIMS Mathematics, 8(1): 2117–2136.
DOI:10.3934/math.2023109
Received: 07 September 2022
Revised: 15 October 2022
Accepted: 23 October 2022
Published: 28 October 2022

http://www.aimspress.com/journal/Math

Research article

Analysis of horizontally polarized shear waves on a highly inhomogeneous loaded bi-material plate

Maha M. Helmi[1], **Ali M. Mubaraki**[1] **and Rahmatullah Ibrahim Nuruddeen**[2,*]

[1] Department of Mathematics and Statistics, College of Science, Taif University, P.O. Box 11099, Taif 21944, Saudi Arabia

[2] Department of Mathematics, Faculty of Science, Federal University Dutse, P.O. Box 7156 Dutse, Jigawa State, Nigeria

* **Correspondence:** Email: rahmatullah.n@fud.edu.ng; Tel: +2349084181812.

Abstract: The current manuscript critically examines the propagation of horizontally polarized shear waves on the dispersion of a highly inhomogeneous thin bonded bi-material plate when a load due to the Winkler's elastic foundation is prescribed. An analytical procedure of solution is deployed for the study; in addition to the exploitation of effective boundary conditions approach for the asymptotic examination. The overall inference of the current study is the realization of the fact that the vibrational displacements in both layers are enhanced by an increase in the inhomogeneity parameter; at the same time lessened with an increment in the foundation parameter. Moreover, a perfect approximation of the dispersion relation has been realized, with its validity extending to almost the entire low-frequency range. Lastly, the influence of the material inhomogeneity has been noted to affect fundamental mode, as against the presence of the foundation parameter which affects the first harmonic curve. More so, an increase in the two parameters narrows the chances of low-frequency propagation.

Keywords: propagation of waves; bi-material plates; inhomogeneous media; analytical procedure; asymptotic approach
Mathematics Subject Classification: 26A33, 73D05

1. Introduction

Propagation of surface waves has been broadly studied in the past and recent literature sequel to its enormous significance in diverse technological formations, comprising both the plane and corrugated media. This significance is notable in a variety of cutting-edge research in the fields of biomechanics, material science, fluid mechanics, coated and composite media, seismology, and vibration control, to mention a few, read [1–8]. Moreover, several other areas of modern engineering

get pleasure from noteworthy consideration by theorists with regards to the vibration and propagation phenomena in different structural shapes and bodies. We mention here the propagation of waves in a functionally graded beam via approximation approach [9], and the nature of the flexural waves in a piezoelectric layer in the presence of an elastic foundation [10]. We also recall the diverse propagation considerations in composite and multi-layered structures – involving various external effects, like inhomogeneity, thermal and magnetic effects, rotation, initial stress, and material contrasts among others, see [11–22] and the references therein. In addition, as the propagation of waves has been tackled in a variety of media; see the famous book of propagation of waves in solid media by Achenbach [23], there has been a number of reported scenarios of some motivating consideration in the classical literature, like the works of Dutta [24] who analyzed the propagation of longitudinal waves in an elastic medium with material inhomogeneity. We also recall the findings of Bhattacharyya and Bera [25] with regard to the propagation of waves in elastic structure amidst random and linear material properties, respectively, via the application of the decomposition approach. More so, a case of a wave vibrating in an inhomogenous rod was equally examined by Ahmad and Zaman [26] both analytically and asymptotically; see also the recent examination of the influence of temporal deviation on a vibrating elastic substrate by Alzaidi et al. [27].

Furthermore, to review some of the important results/literature with regard to the propagation of waves in elastic multi-layered and coated media, we start off by recalling the work of Kaplunov et al. [28] on the dispersion of plane elastic waves on an inhomogeneous three layers panel. There, the propagation of waves was analyzed within the low frequency and long-wave conditions, for the four different material contrasts of typical sandwich panels. We equally recall the work of Dai et al. [29] on the propagation of plane surface waves on a coated half-space. Both examinations given in [28,29] were carried out with the help of the asymptotic analysis method; one would equally read the recent works reported in [30–34] for more consideration, through the help of an asymptotic analysis method. Additionally, Vinh and Linh [35] and Vinh et al. [36] studied the propagation of Rayleigh waves on an orthotropic and isotropic coated media, respectively; for more on the applications and other deliberations on coated media, interested readers could read [37,38] and the references therewith. Besides, we equally recall the new study about the propagation of Love-type surface waves on a coated structure of infinite extents, by Manna et al. [39,40]; cases of coated orthotropic and coated porous anisotropic extended layers were respectively examined in the references. Lastly, Selim and Althobaiti [41] examined the longitudinal wave propagation on a nano-tube over elastic support, using a wave-based approach; see also [42,43] for some relevant studies in the area.

However, as most of the papers so far reviewed in the literature examined the situation of either a single- or inhomogeneous multi-layered structure with constant material properties as in [11,15–17,20,22,28,31–33] via the asymptotic approximation approach, with the exception of a few consideration as in the recent work of Mubaraki et al. [34]; it will be more pertinent to explore the situation of inhomogeneous multi-layered structures with variable-dependent material properties - thereby compounding the inhomogeneity property of the composite media. In this regard, the current manuscript examines the propagation of horizontally polarized shear waves on the dispersion of a highly inhomogeneous thin bi-material plate with a loaded end surface boundary on one end, due to the Winkler elastic foundation, while a stress-free condition is assumed on the other end. An analytical procedure of solution will be used to get hold of exact vibrational displacements and dispersion relation; in addition to the utilization of the asymptotic approximation approach for the derivation

of the approximate dispersion relation. Additionally, the influence of the material inhomogeneity and that of the Winkler elastic foundation will be examined on the propagation of horizontally polarized shear waves on the governing structure. More so, some inference will be deduced in the end, to pave a way for future considerations. Lastly, the organization of the current paper takes the following format: Section 2 presents the formulation of the aiming model. Section 3 derives the exact analytical solution of the model, while Section 4 derives the consequential exact dispersion relation. Section 5 acquires the related cut-off frequency and static equations; while the approximate dispersion relation is determined in Section 6. Moreover, Sections 7 and 8 give the discussion of the obtained results, and the concluding remarks, respectively.

2. Problem statement

Consider a highly inhomogeneous bi-material plate of constant thicknesses h_1 and h_2, occupying the regions $-h_1 \leq x_2 \leq 0$ and $0 \leq x_2 \leq h_2$, respectively. More so, the individual layers of the plate $-$ and $+$ are perfectly joined down the domain $-\infty < x_1 < \infty$ with each other, see Figure 1.

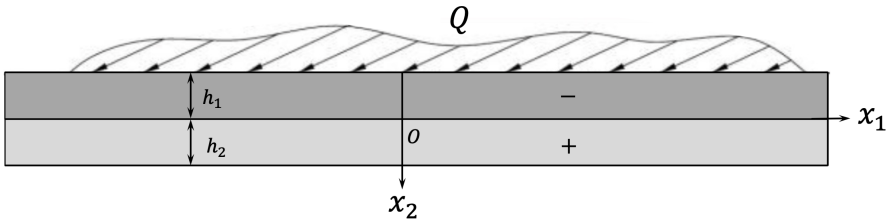

Figure 1. Highly inhomogeneous bi-material plate.

Additionally, we have considered the equation of horizontally polarized shear waves [20,44,45] to describe the propagation of waves in the respective layers of the plate. Horizontally polarized shear motion, or alternatively the anti-plane shear motion has been described by Horgan (1995) [45] as "an interesting two-dimensional mathematical model arising in solid mechanics involving a single second-order linear or quasi-linear partial differential equation. This model has the virtue of relative mathematical simplicity without loss of essential physical relevance. Anti-plane shear deformations are one of the simplest classes of deformations that solids can undergo".

Therefore, the equations of horizontally polarized shear motions, modeling the governing bi-material plate in the displacement $\mathbf{w} = (0, 0, w_3)$ are given in the respective layers as follows [16,20,34]

$$\frac{\partial \tau_{23}^{\mp}}{\partial x_2} + \frac{\partial \tau_{13}^{\mp}}{\partial x_1} = \rho_*^{\pm}(x_2)\frac{\partial^2 w_3^{\mp}}{\partial t^2}, \tag{2.1}$$

where $-$ denotes the upper layer and $+$ denotes the lower layer, $w_3^{\mp} = w_3^{\mp}(x_1, x_2, t)$ are the out-of-plane displacements, $\rho_*^{\mp}(x_2)$ are space-dependent densities; while $\tau_{j3}^{\mp} = \tau_{j3}^{\mp}(x_1, x_2, t)$ are the respective stresses for $j = 1, 2$, and defined by

$$\tau_{j3}^{\mp} = \mu_*^{\mp}(x_2)\frac{\partial w_3^{\mp}}{\partial x_j}, \qquad j = 1, 2, \tag{2.2}$$

where $\mu_*^{\mp}(x_2)$ are space-dependent Lame's elastic parameters. More so, "pure anti-plane shear motions governed by Eq (2.1) are usually called the horizontally polarized shear motion", [23]. Thus, as the

plate is considered to be of a highly inhomogeneous nature, the material constituents comprising the densities $\rho_*^{\mp}(x_2)$ and the Lame's elastic parameters $\mu_*^{\mp}(x_2)$ in the respective layers of the bi-material plate are further presumed to be inhomogeneous, that is, they are x_2-dependents. More specifically, they are represented as follows [27]

$$\rho_*^{\mp}(x_2) = \rho^{\mp}\, e^{-\alpha x_2}, \qquad \mu_*^{\mp}(x_2) = \mu^{\mp}\, e^{-\alpha x_2}, \tag{2.3}$$

where $\rho^{\mp}$ and $\mu^{\mp}$ are the respective constant densities and Lame's elastic parameters, respectively, in the upper and lower plates; while α is the dimensional material inhomogeneity. Moreover, as asserted by Alzaidi et al. [27], the material parameters involving the Lame's constants (shear modulus') $\mu_*^{\mp}(x_2)$ and the material densities $\rho_*^{\mp}(x_2)$ in both layers are considered to have an exponentially decaying variation along their respective thicknesses. Such scenario can be seen as the case of the distribution of material inhomogeneity along the thickness of the structure; take the case of corrosion distribution in an elastic bar [26], or the rate of penetration of an external agent over/across a sheet of metal. In addition, for various considerations of inhomogeneous structures where an exponentially growing variation along the depth of the different elastic media was examined, the recent works by Yigit and Sahin [9] on elastic beams, Mandi et al. [12] on the double-layered structure beneath an inhomogeneous half-plane, and Mubarali et al. [34] on the doubly coated elastic half-plane could be an eye-opener in this regard. More so, some additional material non-homogeneities such as linearly varying material parameters, quadratically material parameters, and exponentially varying material parameters can equally be seen in the work of Shekhar and Parvez. [46]; see also [25–27,34] and the references therewith.

Furthermore, in this regard, there are quite a few other computational methods that compute the wave propagation in highly inhomogeneous materials, such as finite elements, boundary elements, finite difference, and local interaction simulation approach; for such methods, we suggest the reader(s) to read the interesting review work by Shen and Cesnik [47]. In the same vein, it is quite significant to mention the role being played by the concept of dissipation of wave in various media; more on such studies with regard to structure-preserving circumstances can be found in [48–52] and the references therein. Indeed, the dissipation of the wave is an important characteristic of the horizontally polarized shear wave. In the end, however, some work interrelated to the wave vibration of the shells can be found in the recent examinations [53–55].

Furthermore, we prescribe classical conditions that are associated with a typical multi-structure comprising interfacial and boundary conditions as follows

$$\begin{aligned}
&(i) \quad \tau_{23}^{-}(x_1, x_2, t) = -Q, && \text{at} \quad x_2 = -h_1,\\
&(ii) \quad w_3^{-}(x_1, x_2, t) = w_3^{+}(x_1, x_2, t), && \text{at} \quad x_2 = 0,\\
&(iii) \quad \tau_{23}^{-}(x_1, x_2, t) = \tau_{23}^{+}(x_1, x_2, t), && \text{at} \quad x_2 = 0,\\
&(iv) \quad \tau_{23}^{+}(x_1, x_2, t) = 0, && \text{at} \quad x_2 = h_2.
\end{aligned} \tag{2.4}$$

where Q is a tangential load that is considered to be due to an elastic Winkler foundation, which is expressed as [11,34]

$$Q = a\, w_3^{-}. \tag{2.5}$$

where a is the dimensional stiffness of the Winkler's foundation, while w^{-} is the vibrational displacement of the upper layer, where the load is being applied on.

3. Exact analytical solution

In order to solve the governing model, we start off by substituting the constitutive equation expressed in Eq (2.2) in to the equation of motion given in Eq (2.1) to thus obtain the following wave-like equation

$$\frac{\partial^2 w_3^{\mp}}{\partial x_2^2} - \alpha \frac{\partial w_3^{\mp}}{\partial x_2} + \frac{\partial^2 w_3^{\mp}}{\partial x_1^2} = \frac{1}{c_{\mp}^2} \frac{\partial^2 w_3^{\mp}}{\partial t^2}, \tag{3.1}$$

where α is an inhomogeneity parameter, and $c_{\mp}$ are the transverse speeds in the upper and lower regions, respectively, and given by

$$c_{\mp} = \sqrt{\frac{\mu^{\mp}}{\rho^{\mp}}}. \tag{3.2}$$

More so, with the consideration of the harmonic wave solution, we further assume the model to admit the travelling wave solution of the following format [20]

$$w_3^{\mp}(x_1, x_2, t) = u^{\mp}(x_2)\, e^{i(\xi x_1 - \theta t)}, \qquad i^2 = -1, \tag{3.3}$$

where ξ and θ represent the dimensional wavenumber, and frequency, respectively; with the wave propagating along x_1 direction, and x_2 direction represents the thickness direction. Thus, with this development, Eq (3.1) reduces to the following ordinary differential equation

$$\frac{d^2 u^{\mp}}{dx_2^2} - \alpha \frac{du^{\mp}}{dx_2} + \beta_{\mp}^2 u^{\mp} = 0, \tag{3.4}$$

where

$$\beta_{\mp} = \sqrt{\frac{\theta^2}{c_{\mp}^2} - \xi^2}. \tag{3.5}$$

Further, the two equations in Eq (3.4) for the lower and the upper layers pose the following characteristic equations, respectively,

$$m^2 - \alpha m + \beta_-^2 = 0, \quad \text{and} \quad n^2 - \alpha n + \beta_+^2 = 0. \tag{3.6}$$

So, from the above equation, the following roots are obtained

$$m_j = \frac{\alpha + (-1)^j \sqrt{\alpha^2 - 4\beta_-^2}}{2}, \qquad n_j = \frac{\alpha + (-1)^j \sqrt{\alpha^2 - 4\beta_+^2}}{2}, \qquad j = 1, 2. \tag{3.7}$$

Therefore, the exact analytical solution in the upper and lower layers takes the following expression

$$\begin{aligned} w_3^{-}(x_1, x_2, t) &= \left(A^{-} e^{m_1 x_2} + B^{-} e^{m_2 x_2}\right) e^{i(\xi x_1 - \theta t)}, \qquad -h_1 \le x_2 \le 0, \\ w_3^{+}(x_1, x_2, t) &= \left(A^{+} e^{n_1 x_2} + B^{+} e^{n_2 x_2}\right) e^{i(\xi x_1 - \theta t)}, \qquad 0 \le x_2 \le h_2, \end{aligned} \tag{3.8}$$

where $A^{\mp}$ and $B^{\mp}$ are constants to be found right-away after utilising the outlined perfect interfacial and surface boundary conditions.

Therefore, we proceed further by non-dimensionalizing the roots of the characteristic equation expressed in Eq (3.7) as follows

$$m_{jj} = \frac{1}{2}\left(r + (-1)^j \sqrt{r^2 - 4\gamma^2}\right), \qquad n_{jj} = \frac{h}{2}\left(r + (-1)^j \sqrt{r^2 - 4\lambda^2}\right), \qquad j = 1, 2, \tag{3.9}$$

with

$$r = \alpha\, h_1, \qquad \gamma = \sqrt{\Theta^2 - K^2}, \qquad \lambda = \sqrt{\frac{\mu}{\rho}\,\Theta^2 - K^2}, \tag{3.10}$$

where r is the scaled inhomogeneity parameter, and Θ and K are the dimensionless wavenumber and frequency, respectively, given by

$$K = \xi h_1, \qquad \Theta = \frac{\theta h_1}{c_-}, \tag{3.11}$$

together with the dimensionless Lame's elastic parameter μ, density ρ, and thickness h given sequentially as

$$\mu = \frac{\mu_-}{\mu_+}, \qquad \rho = \frac{\rho_-}{\rho_+}, \qquad h = \frac{h_2}{h_1}. \tag{3.12}$$

Moreover, a new dimensionless parameter b is equally discovered denoting the stiffness of the Winkler foundation expressed as

$$b = \frac{a h_1}{\mu_-}. \tag{3.13}$$

Therefore, the respective dimensionless displacements (solutions) and stresses in the two layers of the bi-material plate are determined after ignoring the exponential factor $e^{i(\xi x_1 - \theta t)}$ as follows
displacements $w_3^{\mp}$:

$$\begin{aligned} w_3^- &= h_1\left(e^{m_{11}\zeta_2^-} - \frac{b + m_{11}}{b + m_{22}} e^{-m_{11} + m_{22}(\zeta_2^- + 1)}\right), && -1 \le \zeta_2^- \le 0, \\ w_3^+ &= h_1 R\left(e^{n_{11}\zeta_2^+} - \frac{n_{11}}{n_{22}} e^{n_{11} + n_{22}(\zeta_2^+ - 1)}\right), && 0 \le \zeta_2^+ \le 1, \end{aligned} \tag{3.14}$$

shear stresses $\tau_{13}^{\mp}$:

$$\begin{aligned} \tau_{13}^- &= i\mu^- K e^{r\zeta_2^-}\left(e^{m_{11}\zeta_2^-} - \frac{b + m_{11}}{b + m_{22}} e^{-m_{11} + m_{22}(\zeta_2^- + 1)}\right), && -1 \le \zeta_2^- \le 0, \\ \tau_{13}^+ &= i\mu^+ K R e^{rh\zeta_2^-}\left(e^{n_{11}\zeta_2^+} - \frac{n_{11}}{n_{22}} e^{n_{11} + n_{22}(\zeta_2^+ - 1)}\right), && 0 \le \zeta_2^+ \le 1, \end{aligned} \tag{3.15}$$

shear stresses $\tau_{23}^{\mp}$:

$$\begin{aligned} \tau_{23}^- &= \mu^- e^{r\zeta_2^-}\left(m_{11} e^{m_{11}\zeta_2^-} - \frac{b + m_{11}}{b + m_{22}} m_{22} e^{-m_{11} + m_{22}(\zeta_2^- + 1)}\right), && -1 \le \zeta_2^- \le 0, \\ \tau_{23}^+ &= \mu^+ R n_{11} e^{rh\zeta_2^+}\left(e^{n_{11}\zeta_2^+} - e^{n_{11} + n_{22}(\zeta_2^+ - 1)}\right), && 0 \le \zeta_2^+ \le 1, \end{aligned} \tag{3.16}$$

where

$$R = \frac{n_{22}\left[(b + m_{22})e^{m_{11}} - (b + m_{11})e^{m_{22}}\right]}{(b + m_{22})\left(n_{22}e^{n_{22}} - n_{11}e^{n_{11}}\right)} e^{n_{22} - m_{11}}, \tag{3.17}$$

while ζ_2^- and ζ_2^+ are scaled variables valid over $-h_1 \leq x_2 \leq 0$ and $0 \leq x_2 \leq h_2$, respectively. Additionally, we graphically illustrate in Figure 2 the effects of the (a) inhomogeneity parameter r (with fixed $b = 0.25$), and that of the (b) Winkler foundation parameter b (with fixed $r = 0.25$) on the propagation of horizontally polarized shear waves on the structure under consideration. From these sub-figures, the vibrational displacement in the upper layer ($'-' : -1 \leq \zeta_2 \leq 0$) is observed to decrease steadily down to the prescribed perfect interfacial conditions, which are well satisfied on the interface (at $\zeta_2 = 0$), then followed by an almost linear behavior in the lower layer ($'+' : 0 \leq \zeta_2 \leq 1$) of the plate. Again, one will note from Figure 2(a) that an increase in the inhomogeneity parameter causes an increment in the vibrational displacement; while an increase in the Winkler foundation parameter decreases the vibration, as observed from Figure 2(b).

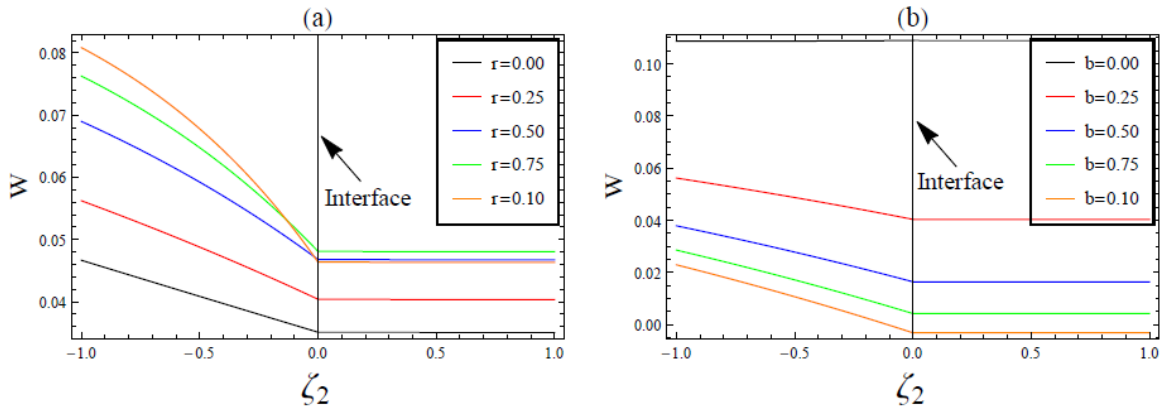

Figure 2. Vibrational effects of the (a) inhomogeneity parameter r, and that of the (b) Winkler foundation parameter b on the propagation of horizontally polarized shear waves determined in Eq (3.14) when $h = 0.8$, $\mu = 1.2$ and $\rho = 1$.

4. Exact dispersion relation

The derivation of the exact dispersion relation is very important in such a structural arrangement comprising of multiply laminated segments. Thus, this section aims to analytically determine the consequential exact dispersion relation with the help of the outlined interfacial and surface conditions.

Now, we determine the consequential exact dispersion relation in this scenario by considering the load Q prescribed in Eq (2.5) on one side of the plate, together with perfect interfacial conditions given in Eq (2.4). Then, the form of interfacial and boundary conditions (including the load condition) yields the following exact dispersion matrix

$$A = \begin{pmatrix} 0 & 0 & (m_{11}+b)e^{-m_{11}} & (m_{22}+b)e^{-m_{22}} \\ n_{11} & n_{22} & -hm_{11} & -hm_{22} \\ 1 & 1 & -1 & -1 \\ n_{11}e^{n_{11}} & n_{22}e^{n_{22}} & 0 & 0 \end{pmatrix}. \tag{4.1}$$

More so, the vanishing point of the determinant of the above dispersion matrix ($\det(A) = 0$) gives the

following consequential dispersion relation

$$\begin{aligned} &e^{n_{22}} n_{22} \left(e^{m_{11}} m_{22}(hm_{11} - n_{11}) + m_{11} e^{m_{22}}(n_{11} - hm_{22})\right)+ \\ &e^{n_{11}} n_{11} \left(m_{11} e^{m_{22}}(hm_{22} - n_{22}) + e^{m_{11}} m_{22}(n_{22} - hm_{11})\right)+ \\ &b(n_{22} e^{m_{11}+n_{22}}(hm_{11} - n_{11}) + n_{11} e^{m_{22}+n_{11}}(hm_{22} - n_{22}))+ \\ &b(n_{11} e^{m_{11}+n_{11}}(n_{22} - hm_{11}) + n_{22} e^{m_{22}+n_{22}}(n_{11} - hm_{22})) = 0, \end{aligned} \tag{4.2}$$

or more explicitly after using the expressions for m_{jj} and n_{jj} given in the Eq (3.9) as follows

$$\begin{aligned} &\sinh\left(\frac{hs_1}{2}\right)\left(r\left(\gamma^2 - \lambda^2\right)\sinh\left(\frac{s_2}{2}\right) + \lambda^2 s_2 \cosh\left(\frac{s_2}{2}\right)\right) + \gamma^2 s_1 \sinh\left(\frac{s_2}{2}\right)\cosh\left(\frac{hs_1}{2}\right) + \\ &\frac{b}{2}\left(\sinh\left(\frac{s_2}{2}\right)\left(rs_1 \cosh\left(\frac{hs_1}{2}\right) + s_1^2 \sinh\left(\frac{hs_1}{2}\right)\right) + s_2 \cosh\left(\frac{s_2}{2}\right)\left(r\sinh\left(\frac{hs_1}{2}\right) + s_1 \cosh\left(\frac{hs_1}{2}\right)\right)\right) = 0, \end{aligned} \tag{4.3}$$

where

$$s_1 = \sqrt{r^2 - 4\lambda^2}, \qquad s_2 = \sqrt{r^2 - 4\gamma^2}. \tag{4.4}$$

Besides, the absence of the material inhomogeneity in the two layers of the plate, that is, when $r = 0$, causes the obtained consequential dispersion relation in Eq (4.3) to further reduce to the following

$$\gamma(\gamma \sin(\gamma)\cos(h\lambda) + \lambda \cos(\gamma)\sin(h\lambda)) + b(\gamma \cos(\gamma)\cos(h\lambda) - \lambda \sin(\gamma)\sin(h\lambda)) = 0, \tag{4.5}$$

where γ and λ are again given in the Eq (3.10).

Obviously, in the case of no load, that is, when $b = 0$, the dispersion relation expressed in Eq (4.3) reduces to

$$\sinh\left(\frac{hs_1}{2}\right)\left(r\left(\gamma^2 - \lambda^2\right)\sinh\left(\frac{s_2}{2}\right) + \lambda^2 s_2 \cosh\left(\frac{s_2}{2}\right)\right) + \gamma^2 s_1 \sinh\left(\frac{s_2}{2}\right)\cosh\left(\frac{hs_1}{2}\right) = 0. \tag{4.6}$$

Moreover, in the absence of material inhomogeneity in the two layers of the plate, that is, when $r = 0$, the obtained consequential dispersion relation above for the highly inhomogeneous bi-material plate with stress-free boundaries further reduces to the following

$$\gamma \sin(\gamma)\cos(h\lambda) + \lambda \cos(\gamma)\sin(h\lambda) = 0. \tag{4.7}$$

Thus, the reduced consequential dispersion relation determined above corresponds to an unloaded inhomogeneous bi-material plate with stress-free faces; of course, the inhomogeneity here is due to the lamination of two homogeneous plates to make a solid bi-material structure.

5. Cut-off frequency and static equation

This section specifically refers to the above-obtained consequential exact dispersion relations by deeply scrutinizing them with regard to their respective cut-off frequencies and static equations. In this regard, the propagation of horizontally polarized shear waves on a highly inhomogeneous bi-material plate under the assumption of low-frequency and long-wave is achieved when [28]

$$\Theta \ll 1, \qquad \text{and} \qquad K \ll 1. \tag{5.1}$$

where Θ and K denote the dimensionless frequency and wave number, respectively; see Eq (3.11) for their explicit expressions. Additionally, interested readers can equally read [17,28] and the references therewith for more related studies concerning the significance of material contrasts.

Hence, in what follows, we determine the cut-off frequency and static equation associated with the governing structure.

5.1. Cut-off frequency

The presence of the scaled inhomogeneity parameter r in the consequential dispersion relation needs to vanish in order to get to the desired target, that is, $r = 0$. Thus, in this case, the reduced dispersion relation given in the Eq (4.5) would be used. Then, the determination of the cut-off frequency requires the dimensionless wavenumber to vanish, that is, $K = 0$. With this, the cut-off frequencies are obtained as follows

$$\begin{aligned}&\Theta\left(\Theta\sin(\Theta)\cos\left(h\Theta\sqrt{\frac{\mu}{\rho}}\right)+\Theta\cos(\Theta)\sqrt{\frac{\mu}{\rho}}\,\sin\left(h\Theta\sqrt{\frac{\mu}{\rho}}\right)\right)+\\&b\Theta\left(\cos(\Theta)\cos\left(h\Theta\sqrt{\frac{\mu}{\rho}}\right)-\sin(\Theta)\sqrt{\frac{\mu}{\rho}}\,\sin\left(h\Theta\sqrt{\frac{\mu}{\rho}}\right)\right)=0,\end{aligned}\tag{5.2}$$

which visibly reveals cut-off at $\Theta = 0$ and additional (ad) one over the transcendental function as

$$\Theta_{ad} \approx \sqrt{\frac{b\rho}{bh\mu - h\mu - \rho}} \ll 1. \tag{5.3}$$

What's more, in the case of no load, that is when $b = 0$, the cut-off frequency determined in Eq (5.2) reduces to the following

$$\Theta\left(\sin(\Theta)\cos\left(h\Theta\sqrt{\frac{\mu}{\rho}}\right)+\cos(\Theta)\sqrt{\frac{\mu}{\rho}}\sin\left(h\Theta\sqrt{\frac{\mu}{\rho}}\right)\right)=0, \tag{5.4}$$

which obviously reveals cut-off frequencies over the low-frequency range of $\Theta \ll 1$, that is at $\Theta = 0$; one would equally find additional roots associated with the transcendental function, possibly numerically!

5.2. Static equation

Again, we determine the static equation for K by setting the dimensionless frequency $\Theta = 0$ in the reduced dispersion relation to obtain

$$K(K\sinh((h+1)K) - b\cosh((h+1)K)) = 0, \tag{5.5}$$

which visibly admits a root at $K = 0$, and an additional and additional (ad) one over the transcendental function as

$$K_{ad} \approx \sqrt{\frac{b}{h+1}}. \tag{5.6}$$

Equally, in the case of no load, that is when $b = 0$, the static equations determined in Eq (5.5) reduces to the following

$$K\sinh((h+1)K) = 0, \tag{5.7}$$

which gives an apparent root at $K = 0$, and extra ones at the zeros of the sine hyperbolic function.

Lastly, the analytically obtained cut-off frequency and static equation as rightly determined in Eqs (5.2) and (5.5) are depicted in Figures 3 and 4, sequentially. More so, one would see the variational effect of the Winkler foundation parameter b on these equations.

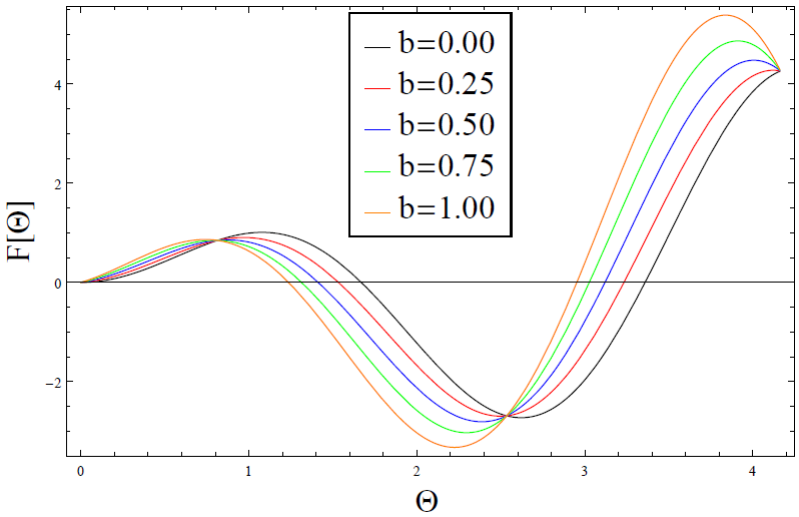

Figure 3. Effect of the Winkler foundation parameter on the analytically obtained cut-off frequency in Eq (5.2) when $h = 0.8$, $\mu = 1.2$ and $\rho = 1$.

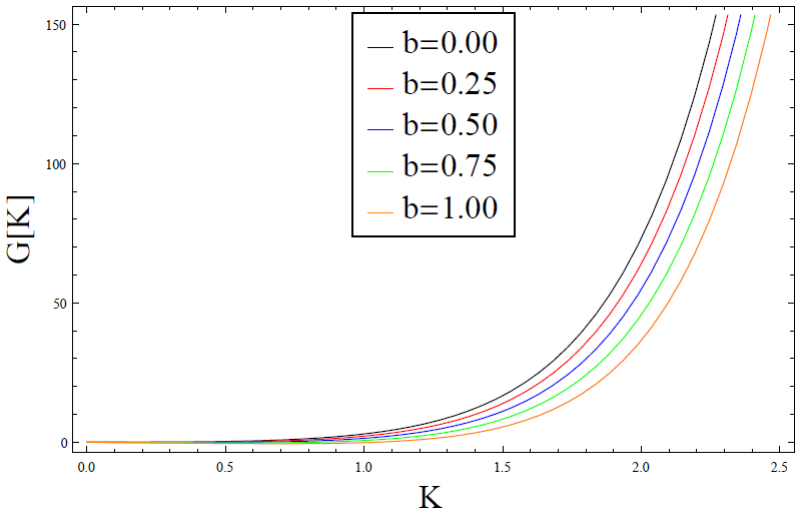

Figure 4. Effect of the Winkler foundation parameter on the analytically obtained static equation in Eq (5.5) when $h = 0.8$, $\mu = 1.2$ and $\rho = 1$.

6. Approximate dispersion relation

The present section makes use of the asymptotic approximation approach, through the application of the effective boundary conditions to derivate the approximate dispersion relation of the earlier determined consequential exact dispersion relation. In doing so, the governing SH equations of motions

would be approximated, and subsequently, get hold of the approximate dispersion relation for the loaded highly inhomogeneous bi-material plate via the stated procedure.

6.1. Treating the upper layer (–)

In this section, the effect of the upper layer − will be analyzed in the long-wave region, that is,

$$K \sim \varepsilon = \frac{h_1}{L} \ll 1,$$

where h_1 is the thickness of the upper layer, and L is the wave length. Thus, we will approximately solve the equation of motion given in Eq (2.1) subject to the boundary conditions expressed in Eq (2.4).

Now, it is appropriate to set the following boundary conditions at the interface ($x_2 = 0$) as follows

$$w_3^- = v^-, \tag{6.1}$$

where the function $v^- = v^-(x_1, t)$ is assumed to be known.

Below, we adopt the asymptotic methodology similar to that for thin elastic structures that was equally used by Mubaraki et al. [32] to approximately analyze an elastic half-space coated by an inhomogeneous layer. With that, let us introduce the following scaling variables

$$\chi = \frac{x_1}{L}, \qquad \eta = \frac{x_2}{h_1}, \qquad \tau = \frac{t\, c_-}{L}, \tag{6.2}$$

and

$$w^* = \frac{w_3^-}{L}, \quad v^* = \frac{v^-}{L}, \quad \tau_{13}^* = \frac{\tau_{13}^-}{\mu^-}, \quad \tau_{23}^* = \frac{\tau_{23}^-}{\varepsilon\,\mu^-}, \quad a^* = \frac{a\,L}{\varepsilon\,\mu^-}, \tag{6.3}$$

where μ^- and ρ^- are constants, $c_- = \sqrt{\frac{\mu^-}{\rho^-}}$ and all quantities with the asterisk are assumed to have the same asymptotic order.

Therefore, with this development, the equation of motion given in Eq (2.1) via the constitutive relations expressed in Eq (2.2) can then be explicitly re-written as

$$\frac{\partial \tau_{23}^*}{\partial \eta} + \frac{\partial \tau_{13}^*}{\partial \chi} = \tilde{\rho}\,(y)\,\frac{\partial^2 w^*}{\partial \tau^2}, \quad \tau_{13}^* = \tilde{\mu}\,(y)\,\frac{\partial w^*}{\partial \chi}, \quad \varepsilon^2\,\tau_{23}^* = \tilde{\mu}\,(y)\,\frac{\partial w^*}{\partial \eta}, \tag{6.4}$$

where

$$\tilde{\rho}\,(y) = \frac{\rho_*^-\,(h_1\eta)}{\rho^-}, \qquad \text{and} \qquad \tilde{\mu}\,(y) = \frac{\mu_*^-\,(h_1\eta)}{\mu^-}. \tag{6.5}$$

Next, the governing boundary conditions become

$$\tau_{23}^* = -a^*\,w^*, \qquad \text{at} \qquad \eta = -1, \quad \text{and} \quad w^* = v^*, \qquad \text{at} \qquad \eta = 0. \tag{6.6}$$

More so, we expand the displacements and stresses involved asymptotically as follows

$$\begin{pmatrix} w^* \\ \\ \tau_{j3}^* \end{pmatrix} = \begin{pmatrix} w^{(0)} \\ \\ \tau_{j3}^{(0)} \end{pmatrix} + \varepsilon \begin{pmatrix} w^{(1)} \\ \\ \tau_{j3}^{(1)} \end{pmatrix} + \ldots, \qquad j = 1, 2. \tag{6.7}$$

Consequently, Eq (6.4) at leading order yields

$$\frac{\partial \tau_{23}^{(0)}}{\partial \eta}+\frac{\partial \tau_{13}^{(0)}}{\partial \chi}=\tilde{\rho}\left(y\right)\frac{\partial^2 w^{(0)}}{\partial \tau^2},\quad \tau_{13}^{(0)}=\tilde{\mu}\left(y\right)\frac{\partial w^{(0)}}{\partial \chi},\quad \frac{\partial w^{(0)}}{\partial \eta}=0, \tag{6.8}$$

subject to the following boundary conditions from Eq (6.6) as follows

$$\tau_{23}^{(0)}=-a^{*}\,w^{(0)},\qquad \text{at}\qquad \eta=-1,\quad \text{and}\quad w^{(0)}=v^{*},\qquad \text{at}\qquad \eta=0. \tag{6.9}$$

Then, the solutions of the above system is found as

$$w^{(0)}=v^{*},\qquad \tau_{13}^{(0)}=\mu_{*}\left(y\right)\frac{\partial v^{*}}{\partial \chi},\qquad \tau_{23}^{(0)}=\left(\int_{-1}^{\eta}\tilde{\rho}\left(y\right)dy\right)\frac{\partial^2 v^{*}}{\partial \tau^2}-\left(\int_{-1}^{\eta}\tilde{\mu}\left(y\right)dy\right)\frac{\partial^2 v^{*}}{\partial \chi^2}-a^{*}\,v^{*} \tag{6.10}$$

Finally, in terms of the original dimensional form, the expressions for the stresses at the interface ($x_2=0$) may be obtained as follows

$$\tau_{23}^{+}=h_1\left[\left(\int_{-h_1}^{0}\rho_{*}^{-}\left(0\right)dx_2\right)\frac{\partial^2 w_3^{+}}{\partial t^2}-\left(\int_{-h_1}^{0}\mu_{*}^{-}\left(0\right)dx_2\right)\frac{\partial^2 w_3^{+}}{\partial x_1^2}\right]-a\,w_3^{+}+O\left(h_1\right). \tag{6.11}$$

More so, as a special case, substituting the exponential inhomogeneity coefficient in Eq (2.3) into Eq (6.11), we arrive at the boundary condition at the interface ($x_2=0$), given as

$$\mu^{+}\frac{\partial w_3^{+}}{\partial x_2}-h_1\,\mu^{-}\left(\frac{1}{c_{-}^2}\frac{\partial^2 w_3^{+}}{\partial t^2}-\frac{\partial^2 w_3^{+}}{\partial x_1^2}\right)-a\,w_3^{+}=0. \tag{6.12}$$

6.2. Asymptotic dispersion relation

Now, having effectively suppressed the effect of the entire upper layer through the boundary condition determined in Eq (6.12), we further make use of the same procedure to re-represent the interfacial and boundary (stress-free) conditions associated with the lower layer earlier prescribed in Eq (2.4) as follows

$$\frac{\partial w_3^{+}}{\partial x_2}-h_1\,\mu\left(\frac{1}{c_{-}^2}\frac{\partial^2 w_3^{+}}{\partial t^2}-\frac{\partial^2 w_3^{+}}{\partial x_1^2}\right)-\frac{\mu\,b}{h_1}\,w_3^{+}=0,\qquad \text{at}\qquad x_2=0,$$

and

$$\frac{\partial w_3^{+}}{\partial x_2}=0.\qquad \text{at}\qquad x_2=h_2, \tag{6.13}$$

Thus, without loss of generality, the aiming approximate consequential dispersion relation is determined as follows

$$n_{22}\left(\gamma^2\mu+n_{11}\right)-n_{11}\left(\gamma^2\mu+n_{22}\right)e^{n_{11}-n_{22}}+b\mu\left(n_{11}e^{n_{11}-n_{22}}-n_{22}\right)=0, \tag{6.14}$$

where n_{11} and n_{22} are defined earlier in Eq (3.9) as $n_{11}=\frac{h}{2}\left(r-\sqrt{r^2-4\lambda^2}\right)$ and $n_{22}=\frac{h}{2}\left(r+\sqrt{r^2-4\lambda^2}\right)$. In addition, we graphically compare the exact and approximate dispersion relation in Figure 5 with regard to the posed fundamental mode. The exactitude between the two curves is perfectly observed.

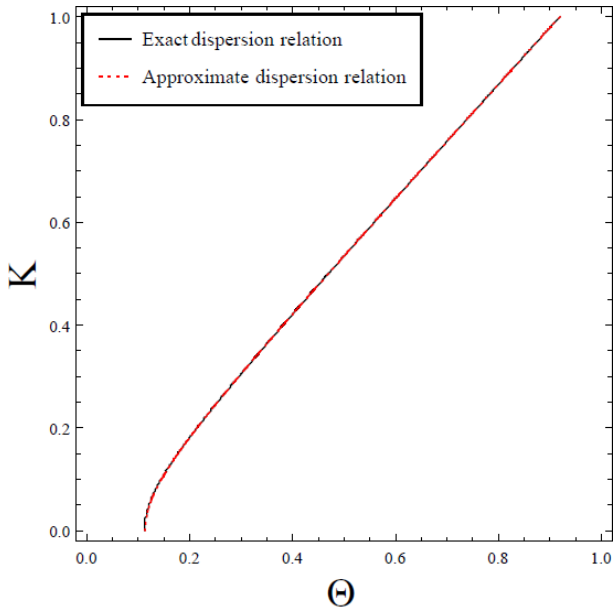

Figure 5. Comparison of the exact dispersion relation Eq (4.3) against the approximate dispersion relation Eq (6.14) when $h = 0.8$, $\mu = 1.2$, $\rho = 1$, $r = 0.25$, and $b = 0.25$.

Hence, having perfectly approximated the obtained consequential exact dispersion relation given in Eq (4.3) by the approximate one as determined in Eq (6.14), we further attempt to graphically show the effect of the inhomogeneity parameter r in Figure 6; while Figure 7 shows the effect of the Winkler foundation parameter b on the propagation of horizontally polarized shear waves via the obtained approximate dispersion relation in Eq (6.14).

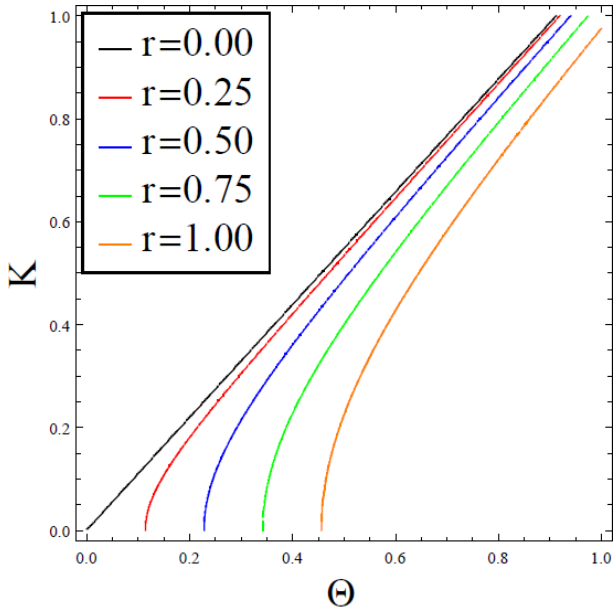

Figure 6. Effect of the inhomogeneity parameter on approximate dispersion relation Eq (6.14) when $h = 0.8$, $\mu = 1.2$, $\rho = 1$, and $r = 0.25$.

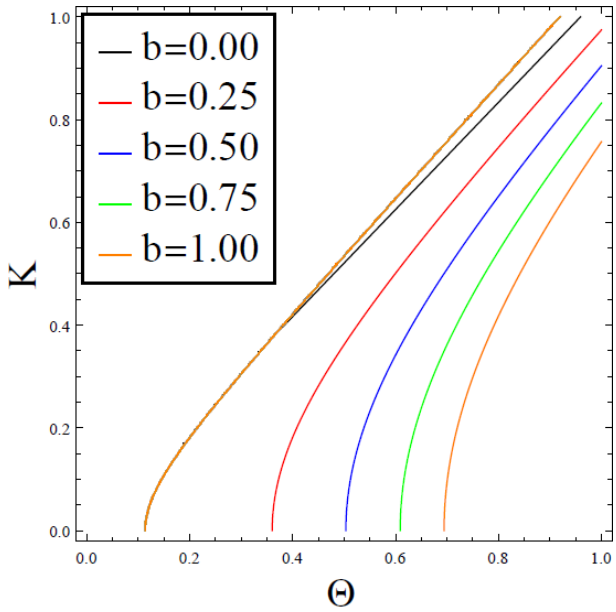

Figure 7. Effect of the Winkler foundation parameter on approximate dispersion relation Eq (6.14) when $h = 0.8$, $\mu = 1.2$, $\rho = 1$, and $r = 0.25$.

7. Discussion of results

The present section attempts to shed more light on the obtained results thereby discussing the effects of the involved parameters on the propagation and dispersion of horizontally polarized shear waves on the bi-material inhomogeneous plate; and on the other hand, discuss the exactitude of the obtained exact and approximate consequential dispersion relations. Recall that the case of a loaded highly inhomogeneous multilayered elastic solid structure is considered, where the upper layer is loaded with a Winkler foundation; moreover, the absence of this foundation (when $b = 0$) rendered the structure to have stress-free faces. Besides, an analytical procedure was primarily utilized for the determination of the analytical solutions, as well as the consequential exact dispersion relations, before the subsequent deployment of the asymptotic procedure by utilizing the effective boundary conditions to determine the equivalent approximate dispersion relations. In addition, such a scenario of varying material properties along the depth of the bi-material plate can be seen as the case of the distribution of material inhomogeneity; take the case of corrosion distribution/spread in an elastic bar or the rate of penetration of an external agent over/across a sheet of metal.

Now, let us begin by discussing the effects of the inhomogeneity parameter r and that of the Winkler foundation parameter b, on the obtained dimensionless vibrational displacements $w^{\mp}$ (see Eq (3.14)) in the respective regions of the plate. This scenario is thus depicted in Figure 2, with 2(a) illustrating the effects of r, while 2(b) illustrates the effects of b, on the upper ($-1 \leq \zeta_2 \leq 0$) and lower ($0 \leq \zeta_2 \leq 1$) layers of the plate. From this figure, it is noted from Figure 2(a) that an increase in the inhomogeneity parameter causes an increment in the vibrational displacement; while an increase in the Winkler foundation parameter decreases the vibration, as observed from Figure 2(b).

In addition, the cut-off frequency and static equation are analytically acquired in Eqs (5.2) and (5.5), sequentially. More so, as the requirement for the existence of these equations, the inhomogeneity

parameter is bound to vanish, thereby allowing only the Winkler foundation parameter to remain. Thus, one would see the variational effects of the Winkler foundation parameter b on these equations as rightly captured in Figures 3 and 4. In addition, as the cut-off frequencies are the roots of the periodic transcendental equations (Eq (5.2)), an oscillatory behavior has been observed upon which the effect of the Winkler foundation parameter continuously sinusoids; while the curves of the static expression increase with an increase in the Winkler foundation parameter.

Next, we discuss Figure 5, which graphically compares the obtained consequential exact and approximate dispersion relation as given in Eqs (4.3) and Eq (6.14), respectively. Recall also that the approximate dispersion relation was determined asymptotically by getting hold of the related effective boundary conditions, and thereafter, derived the approximate equation of motion, which later revealed the approximate dispersion relation in Eq (6.14). Thus, Figure 5 compares the two results by comparing the respective exact and approximate fundamental modes; amazingly, a perfect agreement is realized. Moreover, the selection of the values of the involving parameters ensures a low-frequency harmonic, $\Theta \ll 1$, as the validity for the derived asymptotic equation extends to almost the entire low-frequency range.

Therefore, with the recorded level of exactness between the exact and approximate dispersion curves as shown in Figure 5, we further analyze the effects of the inhomogeneity parameter r in Figure 6, and that of the Winkler elastic foundation parameter b in Figure 7, on the propagation of horizontally polarized shear waves on the governing structure from the derived approximate relation. Hence, from Figure 6, the influence of the inhomogeneity parameter is quite obvious on the vibration – through the fundamental model; take a look at the case when $r = 0$, where the mode propagates at zero. Then, the propagation is followed by a deviation away from the low-frequency region, as the inhomogeneity parameter increases. However, in Figure 7, the effect of the Winkler elastic foundation on the propagation of waves on the governing highly inhomogeneous structure has been noted to be insignificant in the fundamental mode (see the first curve, where all the curves matched on it), as for all the values of b, the propagation remains the same. Nevertheless, the variation is significantly visible on the first harmonic. More so, an increase in the Winkler elastic foundation parameter pushes away the first harmonic from the low-frequency interval.

8. Conclusions

In conclusion, the current manuscript examined the propagation of horizontally polarized shear waves on the dispersion of a highly inhomogeneous thin perfectly bonded bi-material plate with a load due to the Winkler elastic foundation. An analytical procedure of solution was deployed to determine the exact expressions of the consequential vibrational displacements in the two regions of the plate and the respective dispersion relations; in addition to the exploitation of effective boundary conditions for the asymptotic validation of the obtained exact dispersion relations. The vibrational displacements in both layers have been observed to be enhanced by an increase in the inhomogeneity parameter; at the same time lessened with an increment in the foundation parameter. Additionally, a perfect approximation between the exact and approximate dispersion relation has been realized, with the validity for the relation extending to almost the entire low-frequency range. The influence of the material inhomogeneity parameter on the fundamental mode is noted to be obvious, as the more it is increased, the more the deviation away from the low-frequency region. On the other hand, the presence

of the Winkler elastic foundation has been observed to affect the first harmonic mode, in comparison with the inhomogeneity parameter. More so, an increase in the foundation parameter narrowed the chances of low-frequency propagation.

Conflict of interest

The authors declare no conflict of interest.

References

1. J. D. Kaplunov, L. Y. Kossovich, E. V. Nolde, *Dynamics of thin walled elastic bodies*, San Diego, CA: Academic Press, 1998. https://doi.org/10.1016/C2009-0-20923-8
2. I. V. Andrianov, J. Awrejcewicz, V. V. Danishevs'kyy, O. A. Ivankov, *Asymptotic methods in the theory of plates with mixed boundary conditions*, Hoboken, NJ: John Wiley & Sons, Ltd., 2014. https://doi.org/10.1002/9781118725184
3. W. M. Ewing, W. S. Jardetzky, F. Press, Elastic waves in layered media, *Phys. Today*, **10** (1957), 27. https://doi.org/10.1063/1.3060203
4. I. M. Daniel, O. Ishai, *Engineering mechanics of composite materials*, New York: Oxford University Press, 2006.
5. N. P. Padture, M. Gell, E. H. Jordan, Thermal barrier coatings for gas-turbine engine application, *Science*, **296** (2002), 280–284. https://doi.org/10.1126/science.1068609
6. A. Palermo, S. Krodel, A. Marzani, C. Daraio, Engineered metabarrier as shield from seismic surface waves, *Sci. Rep.*, **6** (2016), 39356. https://doi.org/10.1038/srep39356
7. Y. S. Cho, Non-destructive testing of high strength concrete using spectral analysis of surface waves, *NDT & E Int.*, **36** (2003), 229–235. https://doi.org/10.1016/S0963-8695(02)00067-1
8. V. V. Krylov, *Noise and vibration from high-speed trains*, London: Thomas Telford, 2001.
9. G. Yigit, A. Sahin, M. Bayram, Modelling of vibration for functionally graded beams, *Open Math.*, **14** (2016), 661–671. https://doi.org/10.1515/math-2016-0057
10. S. Althobaiti, M. A. Hawwa, Flexural edge waves in a thick piezoelectric film resting on a Winkler foundation, *Crystals*, **12** (2022), 640. https://doi.org/10.3390/cryst12050640
11. B. Erbas, J. Kaplunov, A. Nobili, G. Kilic, Dispersion of elastic waves in a layer interacting with a Winkler foundation, *J. Acoust Soc. Am.*, **144** (2018), 2918–2925. https://doi.org/10.1121/1.5079640
12. A. Mandi, S. Kundu, P. Chandra Pal, P. Pati, An analytic study on the dispersion of Love wave propagation in double layers lying over inhomogeneous half-space, *Journal of Solid Mechanics*, **11** (2019), 570–580.
13. A. M. Abd-Alla, S. M. Abo-Dahab, A. Khan, Rotational effects on magneto-thermoelastic Stoneley, Love, and Rayleigh waves in fibre-reinforced anisotropic general viscoelastic media of higher order, *CMC-Comput. Mater. Con.*, **53** (2017), 49–72. https://doi.org/10.3970/cmc.2017.053.052

14. P. Alam, S. Kundu, Influences of heterogeneities and initial stresses on the propagation of love-type waves in a transversely isotropic layer over an inhomogeneous half-space, *Journal of Solid Mechanics*, **9** (2017), 783–793.

15. S. Althobaiti, A. Mubaraki, R. I. Nuruddeen, J. F. Gomez-Aguilar, Wave propagation in an elastic coaxial hollow cylinder when exposed to thermal heating and external load, *Results Phys.*, **38** (2022), 105582. https://doi.org/10.1016/j.rinp.2022.105582

16. R. I. Nuruddeen, R. Nawaz, Q. M. Zaigham Zia, Effects of thermal stress, magnetic field and rotation on the dispersion of elastic waves in an inhomogeneous five-layered plate with alternating components, *Sci. Progress*, **103** (2020), 1–22. https://doi.org/10.1177/0036850420940469

17. J. Kaplunov, D. A. Prikazchikov, L. A. Prikazchikov, O. Sergushova, The lowest vibration spectra of multi-component structures with contrast material properties, *J. Sound Vib.*, **445** (2019), 132–147. https://doi.org/10.1016/j.jsv.2019.01.013

18. Y. Z. Wang, M. F. Li, K. Kishimoto, Thermal effects on vibration properties of double-layered nanoplates at small scales, *Compos. Part B: Eng.*, **42** (2011), 1311–1317. https://doi.org/10.1016/j.compositesb.2011.01.001

19. S. Kundu, A. Kumari, Torsional wave propagation in an initially stressed anisotropic heterogeneous crustal layer lying over a viscoelastic half-space, *Procedia Engineering*, **173** (2017), 980–987. https://doi.org/10.1016/j.proeng.2016.12.166

20. J. Kaplunov, L. Prikazchikova, M. Alkinidri, Antiplane shear of an asymmetric sandwich plate, *Continuum Mech. Thermodyn.*, **33** (2021), 1247–1262. https://doi.org/10.1007/s00161-021-00969-6

21. J. Vinson, *The behavior of sandwich structures of isotropic and composite materials*, London: Routledge, 2018.

22. M. Asif, R. Nawaz, R. I. Nuruddeen, Dispersion of elastic waves in an inhomogenous multilayered plate over a Winkler elastic foundation with imperfect interfacial conditions, *Phys. Scr.*, **96** (2021), 125026. https://doi.org/10.1088/1402-4896/ac36a1

23. J. D. Achenbach, *Wave propagation in elastic solids, eight impression*, Amsterdam: Elsevier, 1999.

24. A. N. Dutta, Longitudinal propagation of elastic disturbance for linear vibrations of elastic parameters, *Indian Journal of Theoretical Physics*, **4** (1956), 43–50.

25. R. K. Bhattacharyya, R. K. Bera, Application of Adomian method on the solution of the elastic wave propagation in elastic bars of finite length with randomly and linearly varying Young's modulus, *Appl. Math. Lett.*, **17** (2004), 703–709. https://doi.org/10.1016/S0893-9659(04)90108-5

26. F. Ahmad, F. D. Zaman, Exact and asymptotic solutions of the elastic wave propagation problem in a rod, *International Journal of Pure and Applied Mathematics*, **27** (2006), 123–127.

27. A. S. M. Alzaidi, A. M. Mubaraki, R. I. Nuruddeen, Effect of fractional temporal variation on the vibration of waves on elastic substrates with spatial non-homogeneity, *AIMS Mathematics*, **7** (2022), 13746–13762. https://doi.org/10.3934/math.2022757

28. J. Kaplunov, D. Prikazchikov, L. Prikazchikova, Dispersion of elastic waves in a strongly inhomogeneous three-layered plate, *Int. J. Solids Struct.*, **113–114** (2017), 169–179. https://doi.org/10.1016/j.ijsolstr.2017.01.042

29. H.-H. Dai, J. Kaplunov, D. A. Prikachikov, long-wave model for the surface wave in a coated half-space, *Proc. R. Soc. A*, **466** (2010), 3097–3116. https://doi.org/10.1098/rspa.2010.0125

30. A. M. Mubaraki, Asymptotic models for surface waves in coated elastic solids, Ph.D. Thesis of Keel University, Keele, 2021.

31. R. I. Nuruddeen, R. Nawaz, Q. M. Zaigham Zia, Asymptotic approach to anti-plane dynamic problem of asymmetric three-layered composite plate, *Math. Method. Appl. Sci.*, **44** (2021), 10933–10947. https://doi.org/10.1002/mma.7456

32. A. Mubaraki, D. Prikazchikov, A. Kudaibergenov, Explicit model for surface waves on an elastic half-space coated by a thin vertically inhomogeneous layer, In: *DSTA 2019: Perspectives in dynamical systems I: mechatronics and life sciences*, Cham: Springer, 2019, 267–275. https://doi.org/10.1007/978-3-030-77306-9_23

33. A. Mubariki, D. Prikazchikov, On Rayleigh wave field induced by surface stresses under the effect of gravity, *Math. Mech. Solids*, **27** (2022), 1771–1782. https://doi.org/10.1177/10812865221080550

34. A. M. Mubaraki, M. M. Helmi, R. I. Nuruddeen, Surface wave propagation in a rotating doubly coated nonhomogeneous half space with application, *Symmetry*, **14** (2022), 1000. https://doi.org/10.3390/sym14051000

35. P. C. Vinh, N. T. K. Linh, An approximate secular equation of Rayleigh waves propagating in an orthotropic elastic half-space coated by a thin orthotropic elastic layer, *Wave Motion*, **49** (2012) 681–689. https://doi.org/10.1016/j.wavemoti.2012.04.005

36. P. C. Vinh, V. T. N. Anh, V. P. Thanh, Rayleigh waves in an isotropic elastic half-space coated by a thin isotropic elastic layer with smooth contact, *Wave Motion*, **51** (2014), 496–504. https://doi.org/10.1016/j.wavemoti.2013.11.008

37. V. M. Tiainen, Amorphous carbon as a bio-mechanical coating-mechanical properties and biological applications, *Diam. Relat. Mater.*, **10** (2001), 153–160. https://doi.org/10.1016/S0925-9635(00)00462-3

38. M. Li, Q. Liu, Z. Jia, X. Xu, Y. Cheng, Y. Zheng, et al., Graphene oxide/hydroxyapatite composite coatings fabricated by electrophoretic nanotechnology for biological applications, *Carbon*, **67** (2014), 185–197. https://doi.org/10.1016/j.carbon.2013.09.080

39. S. Manna, T. Halder, S. N. Althobait, Dispersion of Love-type wave and its limitation in a nonlocal elastic model of nonhomogeneous layer upon an orthotropic extended medium, *Soil Dyn. Earthq. Eng.*, **153** (2022), 107117. https://doi.org/10.1016/j.soildyn.2021.107117

40. S. Manna, D. Pramanik, S. N. Althobaiti, Love-type surface wave propagation due to interior impulsive point source in a homogenous-coated anisotropic poroelastic layer over a non-homogenous extended substance, *Wave. Random Complex Media*, in press. https://doi.org/10.1080/17455030.2022.2081737

41. M. M. Selim, S. Althobaiti, Wave-based method for longitudinal vibration analysis for irregular single-walled carbon nanotube with elastic-support boundary conditions, *Alex. Eng. J.*, **61** (2022), 12129–12138. https://doi.org/10.1016/j.aej.2022.06.001

42. D. K. Guo, T. Chen, Seismic metamaterials for energy attenuation of shear horizontal waves in transversely isotropic media, *Mater. Today Commun.*, **28** (2021), 102526. https://doi.org/10.1016/j.mtcomm.2021.102526

43. A. M. Mubaraki, S. Althobaiti, R. I. Nuruddeen, Heat and wave interactions in a thermoelastic coaxial solid cylinder driven by laser heating sources, *Case Stud. Therm. Eng.*, **38** (2022), 102338. https://doi.org/10.1016/j.csite.2022.102338

44. C. O. Horgan, K. L. Miller, *Antiplane shear deformations for homogeneous and inhomogeneous anisotropic linearly elastic solids*, *J. Appl. Mech.*, **61** (1994), 23–29. https://doi.org/10.1115/1.2901416

45. C. O. Horgan, Anti-plane shear deformations in linear and nonlinear solid mechanics, *SIAM Rev.*, **37** (1995), 53–81. https://doi.org/10.1137/1037003

46. S. Shekhar, I. A. Parvez, Propagation of torsional surface waves in an inhomogeneous anisotropic fluid saturated porous layered half space under initial stress with varying properties, *Appl. Math. Model.*, **40** (2016), 1300–1314. https://doi.org/10.1016/j.apm.2015.07.015

47. Y. Shen, C. E. S. Cesnik, Hybrid local FEM/global LISA modeling of damped guided wave propagation in complex composite structures, *Smart Mater. Struct.*, **25** (2016), 095021. https://doi.org/10.1088/0964-1726/25/9/095021

48. W. Hu, M. Xu, F. Zhang, C. Xiao, Z. Deng, Dynamic analysis on flexible hub-beam with step-variable cross-section, *Mech. Syst. Signal Proc.*, **180** (2022), 109423. https://doi.org/10.1016/j.ymssp.2022.109423

49. W. Hu, C. Zhang, Z. Deng, Vibration and elastic wave propagation in spatial flexible damping panel attached to four special springs, *Commun. Nonlinear Sci. Numer. Simul.*, **84** (2020), 105199. https://doi.org/10.1016/j.cnsns.2020.105199

50. W. Hu, J. Ye, Z. Deng, Internal resonance of a flexible beam in a spatial tethered system, *J. Sound Vib.*, **475** (2020), 115286. https://doi.org/10.1016/j.jsv.2020.115286

51. W. Hu, M. Xu, J. Song, Q. Gao, Z. Deng, Coupling dynamic behaviors of flexible stretching hub-beam system, *Mech. Syst. Signal Proc.*, **151** (2021), 107389. https://doi.org/10.1016/j.ymssp.2020.107389

52. W. Hu, Y. Huai, M. Xu, Z. Deng, Coupling dynamic characteristics of simplified model for tethered satellite system, *Acta Mech. Sin.*, **37** (2021), 1245–1254. https://doi.org/10.1007/s10409-021-01108-9

53. Y. Dong, X. Li, K. Gao, Y. Li, J. Yang, Harmonic resonances of graphene-reinforced nonlinear cylindrical shells: effects of spinning motion and thermal environment, *Nonlinear Dyn.*, **99** (2020), 981–1000. https://doi.org/10.1007/s11071-019-05297-8

54. Y. Dong, H. Hu, L. Wang, A comprehensive study on the coupled multi-mode vibrations of cylindrical shells, *Mech. Syst. Signal Proc.*, **169** (2022), 108730. https://doi.org/10.1016/j.ymssp.2021.108730

55. M. R. Zarastvand, M. Ghassabi, R. Talebitooti, Acoustic insulation characteristics of shell structures: a review, *Arch. Comput. Methods Eng.*, **28** (2021), 505–523. https://doi.org/10.1007/s11831-019-09387-z

AIMS Press